J Bone Miner Metab (2005) 23[Suppl]:122–131

INVITED PAPER

Yebin Jiang · Jenny Zhao · Er-Yuan Liao · Ru-Chun Dai
Xian-Ping Wu · Harry K. Genant

Application of micro-CT assessment of 3-D bone microstructure in preclinical and clinical studies

Abstract As the mechanical competence of trabecular bone is a function of its apparent density and 3-D distribution, assessment of 3-D trabecular structural characteristics may improve our ability to understand the pathophysiology of osteoporosis, to test the efficacy of pharmaceutical intervention, and to estimate bone biomechanical properties. We have studied ovariectomy-induced osteopenia in rats and its treatment with agents such as estrogen and sodium fluoride. We have demonstrated that 3-D micro-computed tomography (μCT) can directly quantify mouse trabecular and cortical bone structure with an isotropic resolution of $6\mu m^3$. μCT is also useful for studying osteoporosis in mice and phenotypes of mice with gene manipulation, such as SHIP-knockout mice, which are severely osteoporotic due to increased numbers of hyperresorptive osteoclasts, PTHrP heterozygous-null mice, and mice with Zmpste24 deficiency. μCT can quantify osteogenesis in mouse Ilizarov leg-lengthening procedures, osteoconduction in a rat cranial defect model, and structural changes in arthritic rabbits, rats, and mice. In clinical studies, we evaluated longitudinal changes in the iliac crests. Paired bone biopsies from the same premenopausal and postmenopausal women showed the changes in 3-D trabecular structure, such as decreased trabecular thickness, shifting of trabecular model from platelike structure to rodlike structure, and decreased degree of anisotropy were remarkable. Treatment with PTH in postmenopausal women with osteoporosis significantly improved trabecular morphology with a shift toward a more platelike structure, increased trabecular connectivity density, and increased cortical thickness. Paired bone biopsy specimens from the iliac crest in postmenopausal women with osteoporosis before and an average of 2 years after beginning of estrogen replacement therapy demonstrated that posttreatment biopsies showed a significant change in the ratio of plates to rods and statistically insignificant changes in other 3-D trabecular parameters. Thus, μCT can characterize 3-D structure of various animal models, and the longitudinal changes in 3-D bone microarchitectural integrity that deteriorates in the transmenopausal period, is preserved with HRT, and is improved with PTH treatment in postmenopausal women.

Key words Osteoporosis · 3-D microstructure · Estrogen · PTH · Human · Rat · Mouse

Y. Jiang (✉) · J. Zhao · H.K. Genant
Osteoporosis and Arthritis Research Group, Department of Radiology, University of California-San Francisco, San Francisco, CA 94143-0628, USA
Tel. +1-415-502-6651; Fax +1-415-502-6187
e-mail: yebin.jiang@radiology.ucsf.edu

E.Y. Liao · R.C. Dai · X.P. Wu
Institute of Endocrinology & Metabolism, the Second Xiang-Ya Hospital of Central South University, Hunan, China

Introduction

The biomechanical competence of bone, a matrix of mineral and organic materials with a certain architecture and texture, depends on two variables: its geometric properties and its material properties. In terms of fracture risk, decreasing bone mineral leads to an exponential increase in fracture risk. However, other studies have found that bone strength is only partially explained by bone mineral and that bone architecture has great influence on bone strength and the risk of fracture. Bone mineral values in normal and osteoporotic people overlap widely, and the expected correlation between the severity of osteoporosis and the degree of loss in bone mineral has not always been found. The influence of factors other than bone mineral is thought to explain to some extent the overlap in bone mineral measurements between patients with and without osteoporotic fractures. Just as with bridges and buildings, the biomechanical competence or fracture resistance of bone depends not only on the amount of material but also on its spatial distribution, its structure, and its architecture [1,2].

Micro-computed tomography (μCT), an imaging technique originally developed for detecting stress defects in metals in the car industry, has found application in the assessments of 3-D bone microstructure. The μCT system

was first introduced by Feldkamp and Goldstein [3,4], who used a μfocus X-ray tube as a source, an image intensifier as a 2-D detector, and a cone-beam reconstruction to create a 3-D object. Instead of rotating the X-ray source and detectors during data collection as in clinical CT, the specimen is rotated at various angles. X-rays are partially attenuated as the specimen rotates in equal steps in a full circle about a single axis. At each rotational position, the surviving X-ray photons are detected by a planar 2-D array. A 3-D-reconstruction array is created directly in place of a series of 2-D slices.

As the mechanical competence of trabecular bone is a function of its apparent density and 3-D distribution, assessment of 3-D trabecular structural characteristics may improve our ability to understand the pathophysiology of osteoporosis, to test the efficacy of pharmaceutical intervention, and to estimate bone biomechanical properties. 3-D structure is typically inferred indirectly from histomorphometry and stereology on a limited number of 2-D sections based on a parallel plate model [5]. The amount of tissue available for analysis is small, based on only a few thin histological sections of the biopsy core, which may lead to pronounced variation of calculated structural indices and various possible biases. Particularly limiting is the destructive nature of the 2-D histology procedure, which prevents the specimen from being used for other measurements, such as analysis in different planes, and 3-D connectivity density or integrity of trabecular structure, which is highly desirable because of the anisotropic nature of cancellous bone. During aging and in diseases such as osteoporosis, the trabecular plates are perforated and the connecting rods are dissolved, with a continuous shift from one structural type to the other. The introduction of 3-D direct measuring techniques such as μCT in bone research makes it possible to capture the true trabecular architecture without assumptions of the structure type.

Much progress has been made in developing μCT for nondestructive assessment of 3-D trabecular structure and connectivity. The availability of 3-D measuring techniques and 3-D image processing methods allows direct quantification of unbiased morphometric parameters, such as direct volume and surface determination [6], model-independent assessment of thickness [7], and 3-D connectivity estimation [8]. It has found extensive application in the assessment of bone microstructure.

Technical consideration

The segmentation algorithm is important to accurately and reproducibly classify pixels from images in a fast, objective, nonuser-specific manner. Segmentation is usually threshold- or edge based. The threshold depends on the absolute gray value of the pixel, i.e., bone and marrow densities. Global thresholds apply the same threshold to the whole image, which works well in high-resolution and high-contrast images, whereas local thresholds adapt this value to a neighborhood of a selectable size. Edge-based methods apply the first- or second-order derivative and therefore detect changes in gray values [9]. Although some decisions have to be made by the operator, such as placement of the region of interest (ROI), the important advance is that the algorithm is implemented in a uniform manner across all images. An in vitro study showed that precision error as coefficient of variation (CV) and standardized CV of trabecular structural parameters was <5% [10].

A marching cube algorithm has been used extensively for segmenting 3-D bone structure from desktop μCT images and for generation of 3-D surface-rendering images with the smooth surface of 3-D polygonal representation consisting exclusively of triangles [11]. Because the X-ray attenuation throughout a nonhomogeneous material is not uniform and trabeculae of varying densities may exist, the selection of one commonly used global and local gray-scale threshold value, or constraint region growing segmentation method, to create a binary image may not be optimal. With the marching cube algorithm, mineralized bone is separated from bone marrow with a 3-D segmentation algorithm based on the analysis of directional derivatives that is computed from a continuous polynomial fit least squares approximation of the originally discrete CT volume to search for image primitives. Such primitives could be described by different types of digital edges, which are most commonly characterized by intensity changes in a local image neighborhood. For example, roof edges represent points of change from increasing to decreasing intensities or vice versa, whereas step edges describe the borderline between two adjacent regions with different intensities. Bone surface area is determined using the marching cubes method to triangulate the surface of the mineralized bone phase using an interpolating 3-D surface reconstruction algorithm. The marching cube algorithm decides how a logical cube spawned by neighboring voxels is intersected by the surface. The resulting surface is a polygon represented by triangles. A voxel within a cube can either belong to the object or to the background. Various triangulated surfaces result from the intersection of the surface and the cube, depending on the voxel configurations with a cube. The algorithm marches on to the next cube, after detecting the surface of the investigated cube in the discrete dataset. This divide-and-conquer approach allows us to smooth the surface and to obtain a 3-D polygonal surface representation consisting exclusively of triangles.

Bone volume (BV) can be calculated using tetrahedrons corresponding to the enclosed volume of the triangulated surface. Total volume (TV) is the volume of the sample that was examined. To compare samples of varying size, a normalized index, BV/TV, is used. Trabecular thickness is determined by filling maximal spheres in the structure with the distance transformation, then calculating the average thickness of all bone voxels. Trabecular separation is calculated with the same procedure, but the voxels representing nonbone parts are filled with maximal spheres. Separation is the thickness of the marrow cavities. Trabecular number is taken as the inverse of the mean distance between the mid-axes of the observed structure. The midaxes of the structure are assessed from the binary 3-D image using

the 3-D distance transformation and extracting the center points of nonredundant spheres that fill the structure completely. Then, the mean distance between the midaxes is determined similarly to the separation calculation; i.e., the separation between the midaxes is assessed.

The deterioration of trabecular bone structure is characterized by a change from plate elements to rod elements. Consequently, the terms rodlike and platelike are frequently used for a subjective classification of cancellous bone. A new morphometric parameter called the structure model index (SMI) makes it possible to quantify the characteristic form of a 3-D structure in terms of the amount of plates and rods composing the structure. The SMI is calculated by 3-D image analysis based on a differential analysis of the triangulated bone surface. The SMI value is 0 for an ideal plate structure, and 3 for a perfect rod structure or an infinite circular cylinder; round spheres have an SMI of 4. Negative values are the result of pores within bone with high bone volume fractions, indicating a structure with a concave surface resembling Swiss cheese.

Morphological measures such as the Euler characteristic to quantify connectivity, a measure of the maximum number of branches that can be removed before the structure is divided into multiple pieces, can be determined in the μCT dataset without prior skeletonization (Odgaard and Gundersen 1993; Feldkamp et al. 1989). The connectivity, c, of a two-component system such as bone and marrow can be derived directly from the Euler characteristic, e, by $c = 1 - e$ [8], if all the trabeculae and bone marrow cavities are connected without isolated marrow cavities inside the bone. Usually, connectivity is normalized by examined tissue volume and reported as connectivity density in $1/mm^3$. Discrepant results of the connectivity measurements, ranging from highly linear to nonlinear relationships with bone volume, have been reported [3,8,12], which might be due to different specimen and sample sizes studied. Goulet et al. [13] utilized images of bone cubes and related these image-based parameters to Young's modulus, a measure of elasticity of bone. Based on data sets from Feldkamp's μCT, Engelke et al. [14] developed a 3-D digital model of trabecular bone that could be used to compare 2-D and 3-D structural analysis methods and to investigate the effect of spatial resolution and image processing techniques on the extraction of structural parameters.

The geometric degree of anisotropy (DA) is defined as the ratio between the maximal and the minimal radius of the mean intercept length (MIL) ellipsoid. The MIL distribution is calculated by superimposing parallel test lines in different directions on the 3-D image. The directional MIL is the total length of the test lines in one direction divided by the number of intersections with the bone marrow interface of the test lines in the same direction. The MIL ellipsoid is calculated by fitting the directional MIL to a directed ellipsoid using a least squares fit. Also, the relationship of these parameters to in vitro measures of strength and their application to microfinite element modeling has been shown [15].

Trabecular microarchitecture corresponds to the spatial organization of trabeculae. An important microarchitecural property of trabecular bone is the anisotropy of the structure, defined by the existence of preferential direction(s) in the trabecular organization. Anisotropy of trabecular bone tissue primarily involves the preferential orientation(s) of trabeculae and is also reflected by the oriented values of bone strength [16]. Anisotropy is constituted under the influence of strengths applied to bone and permits establishing resistance to these strengths in a given preferential direction. Sugita et al. [16] observed variations in bone strength following the loading directions. These variations were interpreted as an anisotropic feature of the bone strength, and trabecular anisotropy might be considered to predict the fracture risk. The anisotropy of trabecular bone is varying according to the sites. In a study using 2-D imaging technique comparing the properties of calcaneus, distal femur, proximal femur, and vertebrae on human specimens, the highest anisotropy of trabecular bone was found at the calcaneus, followed by distal femur and proximal femur; vertebrae constituted the less anisotropic site [17].

There are currently major research initiatives in the areas of a new μCT scanner for assessment of bone structure, for 3-D structural analysis of small bone samples, or for preclinical and potentially clinical studies. The discrete elements in digital images are called pixels for 2-D and voxels for 3-D. From a physical perspective, spatial resolution is typically given in line pairs per millimeter or as a 5% or 10% value of the modulation transfer function, requiring measuring the modulation transfer function or the point spread function of the imaging system. For simplicity, pixel or voxel dimensions are used, which may result in a "pseudo"-resolution that typically overestimates the physically "correct" resolution by a factor of 2–4. Therefore, to image 50-μm-thick structures the "correct" resolution must be at least 50 μm, requiring pixel/voxel size of 25 μm or smaller according to Nyquist's theorem [9].

These state-of-the-art scanners approach the limits of spatial resolution achievable in vivo with acceptable radiation exposure [18]. The radiation dose can limit spatial resolution and the signal-to-noise ratio that can be optimized for X-ray-based techniques, as theoretical calculations show that a spatial resolution of 100 μm approaches the limit for human in vivo examination [19]. An increase in image resolution by a factor of 2 without an increase in noise will result in an increase of dose by a factor of 8, should slice thickness remain unchanged, whereas dose will be increased by a factor of 16 should slice thickness be further decreased by a factor of 2 [9,20], as the applied surface dose (D) is affected by the resolution (w) and slice thickness (h): $D \approx 1/w^3h$ [9,19]. Contrast, noise, and resolution are all important factors for successful detection of trabecular structure. An increase in noise limits the detectability of finer details of trabeculae. Usually the slice thickness for standard CT is larger than the in-plane pixel size, leading to lower spatial resolution but higher contrast than isotropic resolution, because the pixels representing trabeculae are filled with a larger amount of bone and a smaller amount of marrow as a result of partial volume effect, and because an increase in slice thickness can reduce the noise by a factor of 5 [9].

Applications

The early uses of 3-D μCT focused on the technical and methodological aspects of the systems, but recent developments emphasize the practical aspects of microtomographic imaging. At an early stage, the 3-D cone-beam μCT was used to image the trabecular bone architecture in small samples of human tibias and vertebrae, ex vivo, with a spatial resolution of 60μm [3]. A resolution of 60μm, although acceptable for characterizing the connectivity of human trabeculae, may be insufficient for studies in small animals such as rats where the trabecular widths average about 50μm and trabecular separations average 150μm or less [12]. With the introduction of a desktop μCT device dedicated to the study of bone specimens [21], it has been used extensively in laboratory investigations. Image processing algorithms, free from the model assumptions used in 2-D histomorphometry, have been developed to segment and directly quantify 3-D trabecular bone structure [7,22].

Human samples

Human iliac crest bone has been traditionally assessed with bone histomorphometry based on only a few thin 2-D sections of the biopsy core from limited tissue available, which may result in pronounced variation of calculated structural indices and various possible biases. Analysis of 3-D structure of bone biopsies is now possible using μCT, which permits measurements of the entire biopsy core and therefore may provide more stable and unbiased estimates of bone structural indices.

One recent study compared iliac crest bone samples from premenopausal women with iliac crest bone samples taken from the same women after menopause (Fig. 1). The samples were examined using μCT with an isotropic resolution of $20\mu m^3$. The postmenopause samples showed significant changes in 3-D trabecular structural parameters. The annual rate of change from platelike structure to rodlike structure was 12%, which may have important consequences for bone biomechanical properties. Trabecular bone became more isotropic after menopause, with an annual decrease rate in DA of 0.7%. Interestingly, annual change in trabecular thickness (−3.5%) is greater than the change in trabecular number (−1.6%) and separation (+2%) [23]. These findings are quite different from those of traditional 2-D histomorphometry. In histomorphometry, it is still a matter of debate whether trabeculae thin or simply disappear after menopause and with aging. It is possible that the loss of entire elements because of trabecular perforation forms the main mechanism of structural changes in osteoporosis. The remaining trabeculae are more widely separated and some may undergo compensatory thickening. Trabecular anisotropy will increase. During the early stages of aging in the human, there is a preferred loss of horizontal trabeculae, leading to an increase in anisotropy [24], followed by a period of trabecular perforation and an eventual decrease in anisotropy.

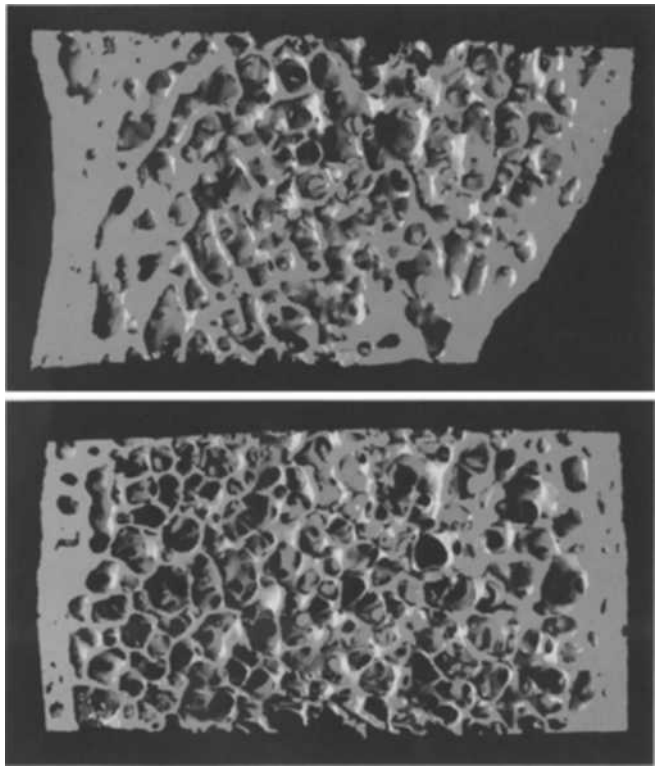

Fig. 1. Two paired iliac crest bone biopsy samples from one woman. The first biopsy was taken when she was healthy, premenopausal, and 53 years old. The second biopsy was from the opposite side, 5 years later, after menopause. The samples were examined using microcomputed tomography (μCT) with an isotropic resolution of $20\mu m^3$. The trabecular structure is mainly platelike and quite anisotropic in general before menopause (*upper*). The changes in three-dimensional (3-D) trabecular structure after menopause (*bottom*) are dramatic: 3-D trabecular bone volume has decreased, trabecular separation has increased, the trabeculae have become thinner and more isotropic, and there has been a shift from platelike to rodlike structure

In our analysis, the changes of more simple 2-D indices pertaining to cancellous bone structure, trabecular number (Tb.N), trabecular thickness (Tb.Th), and trabecular spacing (Tb.Sp) did not reach significance after parathyroid hormone (PTH) treatment. However, more stereologically correct indices, such as marrow star volume and μCT-based 3-D indices, revealed significant changes, further corroborating the superiority of these techniques for structural analysis of small samples such as bone biopsies. To determine the reproducibility of μCT examination, 20 specimens from different groups were rescanned and reanalyzed. The root mean square CV of the measurements was 2.6% for Tb bone volume fraction (BV/TV), 3.6% for Tb number, 5.9% for Tb thickness, 4.0% for Tb separation, 3.3% for Tb degree of anisotropy, 2.1% for SMI, 3.9% for Tb connectivity density (CD), 2.7% for cortical porosity (Ct.Po), and 2.9% for cortical thickness (Ct.Th). The annualized median percent change in the placebo group was −3.3% for BV/TV, 4.6% for SMI, −9.2% for CD, and −14% for Ct.Po, and in the PTH-treated group 4.7% for BV/TV, −8% for SMI, 13% for CD, 0.5% for Ct.Po, and 14% for Ct.Th. Thus, micro-CT can reproducibly quantify 3-D microarchitecture

of the trabecular and cortical bone in iliac crest biopsy, which may find application in studying the pathophysiology of osteoporosis and other bone disorders and evaluating their therapeutic efficacy [25].

μCT has been used in evaluating 3-D bone microstructure of bone biopsies from patients treated with antiresorptive agents such as estrogen [26], and bisphosphonate residronate, which preserves bone microstructure in postmenopausal osteoporotic women [27]. We examined bone biopsy specimens from the iliac crest in postmenopausal women with osteoporosis before and an average of 2 years after beginning of estrogen replacement therapy (ERT). Bone biopsies were obtained from one side of the iliac crest before treatment and from the other side after treatment. Compared to pretreatment biopsies, posttreatment biopsies showed a 14% change in the ratio of plates to rods, but statistically insignificant changes in trabecular bone volume, thickness, number, separation, and connectivity density. The findings indicate that ERT not only preserves existing three-dimensional trabecular bone microarchitecture, but that it also reverses the shift from the platelike to rodlike pattern that is characteristic of osteoporosis. This reversal may reduce the risk of fractures due to osteoporosis by increasing the biomechanical competence of bone [26].

In addition to the studies of antiresorptive agents, μCT has also been used in evaluating 3-D bone microstructure of bone biopsies from patients treated with anabolic agents. In an uncontrolled study of paired biopsies taken before and after treatment with human PTH, 3-D μCT showed increased 3-D connectivity density and confirmed the preservation of 2-D histomorphometric cancellous bone volume and trabecular number and thickness. Cortical width from 2-D histomorphometry increased in osteoporotic men treated with PTH and in osteoporotic women treated with PTH and estrogen [28].

In a multicenter, double-blind, and placebo-controlled study, once-daily administration of PTH, the major hormonal regulator of calcium homeostasis, caused increased bone formation and bone mass. After the first report in 1929 of increased skeletal calcium in rats after injection of parathyroid extract, preclinical studies and small clinical trials have shown pronounced anabolic effects of intermittent PTH administration on bone. The effect of injected PTH on human cortical bone is controversial. Some small early clinical studies found that appendicular bone mineral density (BMD) was reduced by PTH treatment whereas vertebral BMD increased. In other studies, BMD at the predominantly distal radius or femoral neck changed little during PTH administration. These findings led to speculation that the anabolic effects of teriparatide on cancellous bone may be obtained at the expense of cortical bone. Most recently, a large randomized double-blind multicenter study, the Fracture Prevention Trial, tested recombinant human PTH (1-34) [teriparatide, rhPTH (1-34), TPTD] versus placebo, for treatment of osteoporosis in 1637 postmenopausal women. Daily injections of 20 μg or 40 μg teriparatide over a mean of 19 months increased BMD at the lumbar spine and proximal femur and significantly decreased the incidence of vertebral and nonvertebral fractures. We examined 51 paired iliac crest biopsy specimens of sufficient quality for analysis (choosing from 102 patients in the biopsy study) from subjects participating in this randomized, multicenter, double-blind, placebo-controlled Fracture Prevention Trial in which postmenopausal women with osteoporosis from 99 centers in 17 countries participated. By 2-D histomorphometric analyses, teriparatide significantly increased cancellous bone volume and reduced marrow star volume. PTH was not associated with osteomalacia or woven bone, and there were no significant changes in mineral appositional rate or wall thickness. By 3-D cancellous and cortical bone structural analyses, PTH significantly decreased the cancellous structure model index, increased cancellous connectivity density, and increased cortical thickness. PTH improved trabecular morphology with a shift toward a more platelike structure. These changes in cancellous and cortical bone morphology should improve biomechanical competence and are consistent with the substantially reduced incidences of vertebral and nonvertebral fractures (Fig. 2) [11].

Rat studies

μCT has been used to measure trabecular bone structure in rats. Most studies have focused on the trabecular bone in the proximal tibial metaphysis, but the trabecular bone in rat vertebrae is of interest because of its similarity to the human fracture site and because biomechanical testing is practical [29]. μCT with an isotropic resolution of 11 μm^3 has been used to examine the 3-D trabecular bone structure of the vertebral body (Fig. 3) in ovariectomized rats treated with ERT [30]. μCT 3-D determined trabecular parameters show greater percent-age changes than those observed with dual-energy X-ray absorptiometry (DXA), and they show better correlation with biomechanical properties. Combin-

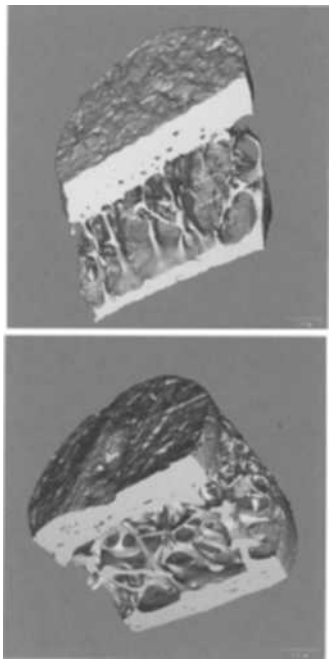

Fig. 2. Three-dimensional μCT reconstructions of a paired iliac crest bone biopsy. Compared to the baseline biopsy (*upper*), treatment with 20 μg parathyroid hormone (PTH) (*bottom*) increased trabecular bone volume, trabecular connectivity, and cortical thickness. Note also the change in trabecular morphology from a rodlike structure to a more platelike pattern in the posttreatment biopsy. This paired biopsy sample was obtained from a 65-year-old woman who was treated with 20 μg PTH for 21 months

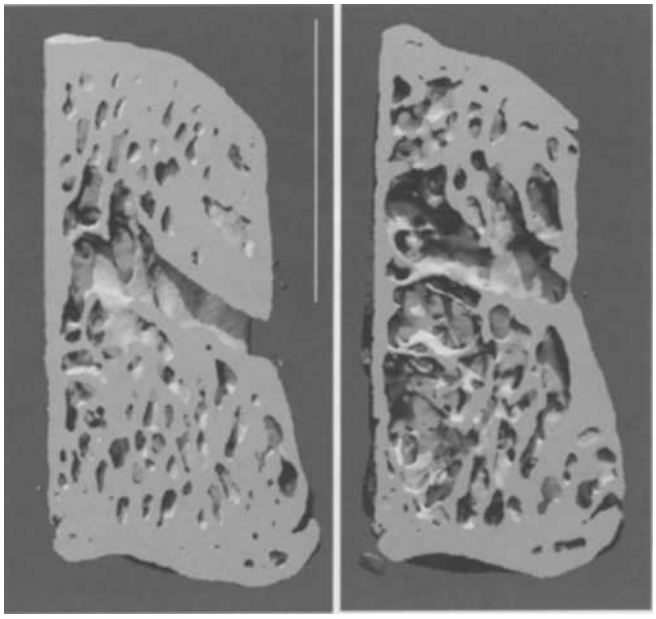

Fig. 3. μCT 3-D images of rat vertebral body with isotropic resolution of 11 μm^3. Compared with age-matched sham-operated control (*left*), ovariectomy results in a remarkable decrease in the trabecular bone volume, thickness, number, and a conspicuous increase in trabecular separation. The different trabecular patterns are noticeable, i.e., plate-like trabeculae in the control and rodlike trabeculae in the ovariectomized rat. Cortical thickness is also decreased after ovariectomy

ing trabecular bone volume with trabecular structural parameters provides better prediction of biomechanical properties than either alone. A study of the anabolic effects of low-dose (5 ppm in drinking water) long-term (9 months) sodium fluoride (NaF) treatment in intact and ovariectomized rats showed that NaF treatment increases trabecular bone volume, possibly by increasing trabecular thickness through increasing bone formation on existing trabeculae, rather than by increasing trabecular number. NaF in sham-operated rats increases trabecular structural parameters and bone mineral, but decreases compressive stress in the vertebral body. NaF partially protects against ovariectomy-induced changes in bone mineral and structure, but this protection does not translate into a corresponding protection of bone biomechanical properties [31,32].

Mice studies

The wide availability of genetically altered mice has increased the usefulness of the murine model for investigating osteoporosis and other skeletal disorders. Independent genetic regulation of 3-D vertebral trabecular microstructure in 12BXH recombinant inbred mice as measured by μCT contributed information regarding the variation in biomechanical properties among the strains [33]. Mice homozygous for a null mutation of the PTHrP gene die at birth with severe skeletal deformities. Heterozygotes survive and by 3 months of age develop osteopenia characterized by decreased trabecular bone volume and increased bone marrow adiposity. PTHrP wild-type and heterozygous-null mice were ovariectomized at 4 months of age and killed at 5 weeks. 3-D μCT was used to examine the trabecular structure of the mice, with an isotropic resolution of 9 μm^3. Bone specimens from mice heterozygous for the PTHrP null allele demonstrate significant changes as compared to wild-type littermates in most parameters examined. However, measurements of trabecular number and trabecular thickness were not significantly different between the two groups. These findings support the notion that PTHrP haploinsufficiency leads to abnormal bone formation in the adult mouse skeleton [34].

The hematopoietic-restricted protein Src homology 2-containing inositol-5-phosphatase (SHIP) blunts phosphatidylinositol-3-kinase-initiated signaling by dephosphorylating its major substrate, phosphatidylinositol-3,4,5-trisphosphate. SHIP−/− mice contain increased numbers of osteoclast precursor macrophages and osteoclast number due to the prolonged life span of these cells and to hypersensitivity of precursors to macrophage colony-stimulating factor (M-CSF) and RANKL. Similar to pagetic osteoclasts, SHIP−/− osteoclasts are enlarged, containing upward of 100 nuclei, and exhibit enhanced resorptive activity. Moreover, as in Paget disease, serum levels of interleukin 6 are markedly increased in SHIP−/− mice. Consistent with accelerated resorptive activity, 3-D trabecular volume fraction, trabecular thickness, and number and connectivity density of SHIP−/− long bones are reduced, resulting in a 49% decrease in biomechanical properties, indicating that SHIP negatively regulates osteoclast formation and function and that the absence of this enzyme results in severe osteoporosis [35]. Zmpste24 is an integral membrane metalloproteinase of the endoplasmic reticulum. The most striking pathological phenotype of Zmpste24 deficiency in mice is multiple spontaneous bone fractures, akin to those occurring in mouse models of osteogenesis imperfecta. There is a significant loss in 3-D bone microstructure of both cortical and trabecular bone in Zmpste24 −/− mice compared with wild-type mice [36].

The physiological role of BMP signaling in bone formation in postnatal life remains undefined. Trabecular bone volume, osteoblast numbers, and bone formation rates in proximal tibiae were reduced 27%, 38%, and 44%, respectively, in Smad1 gene knokout mice compared with control littermates. 3-D micro-CT examination showed that, in tibiae and femora, trabecular volume, number, thickness, and connectivity density were decreased and trabecular separation was increased. In the dnBMPR transgenic mice, there was an identical phenotype to that observed in the Smad1gene knokout mice, namely blockage of bone morphogenetic protein (BMP) signaling, decreased trabecular bone volume, and decreased bone formation rates. These results demonstrate that Smad1 is necessary for normal postnatal bone formation and suggest that BMPs exert their effects on bone formation through the Smad1 signaling pathway [37].

Because of the increasing technical ability to manipulate and study gene expression in the mouse, there is a growing interest in and use of the aged mouse as an animal model to

study age-related bone loss in humans. Indeed, because of the remarkable differences in peak bone mass across mouse strains, much work is now concentrated on seeking genetic loci associated with high and low bone mass. However, the question arises as to whether mice lose bone with age or with deprivation of estrogen and, if so, whether the pattern of loss and change in bone architecture is similar to that in human aging. We have shown that ovariectomy induces short-term high-turnover accelerated deterioration of 3-D trabecular structure in mice. In a study using 3-month-old Swiss Webster mice 5 and 13 weeks after ovariectomy, 3-D μCT trabecular structure was measured in the secondary spongiosa of the distal femur with an isotropic resolution of $9\,\mu m^3$. The trabeculae become more rodlike and more isotropic, thinner, and more widely separated after ovariectomy (Fig. 4) [38]. HRT prevented ovariectomy-induced bone loss. Percentage changes in peripheral quantitated CT (pQCT) volumetric BMD were similar to the changes measured by μCT but less pronounced.

Other research applications

μCT has other research applications, for example, finite-element modeling for evaluation of bone biomechanical properties [39], assessment of bone tumors and treatment response, quantifying osteogenesis in mouse Ilizarov leg-lengthening procedures, and quantifying osteoconduction in a rat cranial defect model. In a model of rheumatoid arthritis in mice, μCT can quantify the loss as a result of erosion and increased bone resorption and treatment response. Destruction of cartilage and bone are hallmarks of poorly managed human rheumatoid arthritis (RA). Because p38·MAP kinase has been shown to modulate the activity of key proinflammatory pathways in RA, we have shown that oral administration of p38 MAP kinase blockade, an inhibitor of this kinase (SD-282), prevents 3-D bone destruction in the early- and late-stage mouse model of a RA model induced with bovine type II cartilage (100 μg/kg, subcutaneous on days 0 and 21) and lipopolysaccharide (50 μg/mouse, intraperitoneal on day 22). In a model of osteoarthritis in dogs, μCT with a nominal resolution of 66 μm was used to examine the subchondral bone changes. 3-D μCT and 2-D histomorphometry showed a decrease in bone volume fraction and an increase in bone surface fraction in the femur and patella of dogs 3 and 6 months, respectively, after an anterior cruciate ligament transection. Histomorphometry also shows an increase in bone formation rate. μCT images of the femur showed multiple pits on the bone surface of femoral condyles and femoral trochlear ridges, whereas gross inspection of the cartilage showed only a discoloration in the corresponding areas, indicating that the subchondral bone erosions preceded articular cartilage damage in the development of osteoarthritis [40].

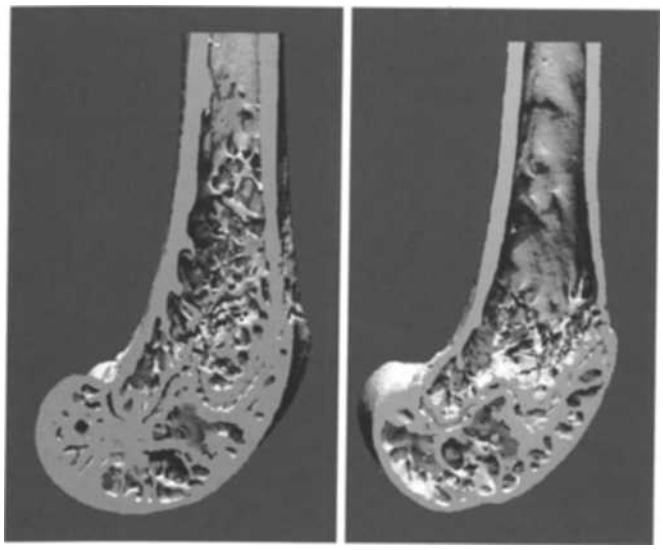

Fig. 4. μCT 3-D images of trabecular and cortical bone structure of mice with isotropic resolution of $9\,\mu m^3$. Compared with age-matched sham-operated control (*left*), ovariectomy results in a draumatic loss of trabecular bone volume and other trabecular bone microstructure (*right*)

Synchrotron radiation

The μCT method was further enhanced by resorting to synchrotron radiation with a spatial resolution of 2 μm [41], or with applications to live rats [12]. Compared with an X-ray tube, the X-ray beam from synchrotron radiation has high magnitude of intensity, monochromaticity, high photon flux, and small angular source size. For X-ray tube μCT, Smith and Silver [42] have reported that 3-D images from cone-beam scanners are inevitably distorted away from the central slice because the single-orbit cone-beam geometry does not provide a complete data set. These distortions and associated loss of spatial resolution have been particularly evident in samples containing platelike structures, even when the cone-beam angle is less than 6.5° [42]. A recent study with direct comparison of fan beam (obtained on the central plane) and cone bone (obtained from a divergent section near the periphery of the volume) techniques over a full cone angle of 9°, using a 100-μm μfocus X-ray tube and isotropic 33-μm voxels, showed that the bone volume fraction based on a gray-scale threshold in excised lumbar vertebrae from normal adult rats was not adversely affected by cone-beam acquisition geometry for cone angles typically used in μCT [43].

The use of the synchrotron radiation X-ray source was first suggested by Grodzins [44] for high-resolution microtomography of small samples. It provides a continuous energy spectrum with a high photon flux. The optimum energy for a given sample can be selected from the synchrotron radiation white beam with a small energy bandwidth (0.1%–0.001%) using a crystal monochromator, while at the same time keeping the photon flux rate high enough for efficient imaging. The monochromaticity of the beam is very important; conventional polychromatic X-ray sources result in beam hardening artifacts in the reconstructed images due to the stronger attenuation of the soft X-ray in the sample. The monochromaticity of the beam is especially important to perform accurate density measurement. The

high photon flux available and small angular source size from synchrotron radiation X-ray sources lead to negligible geometric blur, making it possible to obtain images with high spatial resolution and high signal-to-noise ratio. The X-ray intensity of synchrotron radiation is higher in magnitude than that of X-ray tubes. When scanning time is important, and for resolution less than 1–5 μm, synchrotron radiation is a better choice than X-ray tubes. Adaptation of the X-ray energy to the sample can be optimized by using monochromatic radiation because of the continuous X-ray spectrum of synchrotron radiation, which can minimize radiation exposure for examining small animals in vivo. Synchrotron μCT has spatial resolutions of 2 μm because of the high brightness and natural collimation of the radiation sources [41]. It uses parallel beam imaging geometry, avoids the distortions and loss of resolution inherent in cone-beam methods, and can make distortion-less images of human trabecular bone using a CT at a synchrotron electron storage ring [41]. Recently, μCT using high-intensity and tight collimation synchrotron radiation that achieves a spatial resolution of 1–2 μm has provided the capability to assess additional features such as resorption cavities [45].

Synchrotron μCT at 23 μm/voxel in the proximal tibial metaphysis of live rats [46,47] shows that trabecular connectivity decreased 27% by days 5 and 8 post-ovariectomy and continued to decrease up to day 50 after ovariectomy. The trabecular BV/TV decreased 25% by 8 days after ovariectomy and continued to decrease through day 50. These changes were more rapid than biochemical markers. ERT initiated at 5–13 days after ovariectomy can restore BV/TV – but not connectivity – to baseline levels by allowing bone formation to continue in previously activated bone remodeling units while suppressing the production of new remodeling units. Intermittent hPTH (1-34) treatment in osteopenic ovariectomized rats increased trabecular BV/TV to control levels or higher by thickening existing trabeculae. hPTH (1-34) did not reestablish connectivity when therapy was started after 50% of the trabecular connectivity was lost. At 120 days after ovariectomy, there was a small but significant decrease in trabecular bone volume and a significant decrease in trabecular plate thickness. The decrease in trabecular thickness was associated with an increase in connectivity, in contrast to the proximal tibia where connectivity always declines [48].

In addition, synchrotron radiation X-ray microtomography (μT) using new X-ray optic components has been designed to assess the ultrastructure of individual trabeculae with a resolution of 1 μm and to describe microscopic variations in mineral loading within the bone material of an individual trabecular rod. Artifacts from X-ray refraction and diffraction require methods different from those used for other μCT techniques. Delicate and minimal individual trabecular specimen handling and no microtome cutting preserve the specimen geometry and internal microfractures. The histological features of the mineral ultrastructure can be evaluated using volumetric viewing. The volume, shape, and orientation of osteocyte lacunae and major cannaliculae can be observed. Quantitative measures of trabecular ultrastructure are now being considered including BMU (basic multicellular unit of bone remodeling with activation → resorption → formation sequence) volume, lamellar thickness, and density gradients [49].

The hardware for synchrotron radiation μCT, however, is not readily accessible. Electron storage rings are stationary and cannot be operated in a small laboratory, and only a few synchrotron radiation centers are available worldwide.

Summary

Many studies have shown that changes in bone quality and structural characteristics lead to changes in bone biomechanical competence or individual risk of fracture independently of BMD. Structural measurements using μCT 3-D assessment contribute to our understanding of osteoporosis and other bone disorders and provide insight into their pathomechanisms and treatment response in various animal models and in humans. Although a commercial in vivo animal μCT scanner and a potential clinical micro-CT scanner for measuring bone structure of the distal radius and distal tibia have been developed, most μCT studies are performed in the specimens, mainly because of consideration of higher resolution and radiation exposure.

Although μCT is demanding in terms of equipment and technique, it is unbiased, free from the model assumptions used in 2-D histomorphometry. Because a true 3-D assessment of the trabecular bone structure is possible, rod or plate model assumptions are no longer necessary. μCT devices are able to directly measure 3-D structure, connectivity, and integrity in a highly automated, fast, objective, nonuser-specific manner, with little sample preparation, allowing greater numbers of samples for unbiased comparisons between controls and subjects. They can handle large sample sizes and therefore have less sampling error. They are non-destructive, which allows multiple tests such as biomechanical testing and chemical analysis on the same sample, and noninvasive, which may permit longitudinal studies. These methods also have weaknesses: they require robust image processing algorithms to segment and quantify bone structure, and they may have limitations in spatial resolution for certain structures. They cannot provide information on cellular activities or on dynamic mineralization processes. Rather than replacing bone histomorphometry, these imaging methods provide additional and valuable information and are a useful complement to traditional techniques in the evaluation of osteoporosis and other bone disorders.

References

1. Jiang Y, Zhao J, Genant HK (2002) Macro and micro imaging of bone architecture. In: Bilezikian JP, Raisz LG, Rodan GA (eds) Principles of Bone Biology, 2nd edn. Academic. San Diego, pp 1599–1623

2. Jiang Y, Zhao J, Geusens P, Liao EY, Adriaensens P, Gelan J, Azria M, Boonen S, Caulin F, Lynch JA, Xiaolong Ouyang X, Genant HK (2005) Femoral neck trabecular microstructure in ovariectomized ewes treated with calcitonin: MRI microscopic evaluation. J Bone Miner Res 20:125–130
3. Feldkamp LA, Goldstein SA, Parfift AM, Jesioil G, Kleerekoper M (1989) The direct examination of three-dimensional bone architecture in vitro by computed tomography. J Bone Miner Res 4:3–11
4. Kuhn JL, Goldstein SA, Feldkamp LA, Goulet RW, Jesion G (1990) Evaluation of a microcomputed tomography system to study trabecular bone structure. J Orthop Res 8:833–842
5. Parfitt AM, Matthews C, Villanueva A (1983) Relationships between surface, volume and thickness of iliac trabecular bone in aging and in osteoporosis. J Clin Invest 72:1396–1409
6. Guilak F (1994) Volume and surface area of viable chondrocytes in situ using geometric modeling of serial confocal sections. J Microsc 173:245–256
7. Hildebrand T, Ruegsegger P (1997) A new method for the model independent assessment of thickness in three-dimensional images. J Microsc 185:67–75
8. Odgaard A, Gundersen HJG (1993) Quantification of connectivity in cancellous bone, with special emphasis on 3-D reconstruction. Bone 14:173–182
9. Engelke K, Kalender W (1998) Beyond bone densitometry: assessment of bone architecture by x-ray computed tomography at various levels of resolution. In: Genant HK, Guglielmi G, Jergas M (eds) Bone Densitometry and Osteoporosis. Springer, Berlin, pp 417–447
10. Jiang Y, Zhao J, Augat P, Ouyang X, Lu Y, Majumdar S, Genant HK (1998) Trabecular bone mineral and calculated structure of human bone specimens scanned by peripheral quantitative computed tomography: relation to biomechanical properties. J Bone Miner Res 13:1783–1790
11. Jiang Y, Zhao J, Mitlak BH, Wang O, Genant HK, Eriksen EF (2003) Recombinant human parathyroid hormone (1-34) (teriparatide) improves both cortical and cancellous bone structure. J Bone Miner Res 18:1932–1941
12. Kinney JH, Lane NE, Haupt DL (1995) In vivo, three-dimensional microscopy of trabecular bone. J Bone Miner Res 10:264–270
13. Goulet RW, Goldstein SA, Ciarelli MJ, Kuhn JL, Brown MB, Feldkamp LA (1994) The relationship between the structural and orthogonal compressive properties of trabecular bone. J Biomech 27:375–389
14. Engelke K, Song SM, Glüer CC, Genant HK (1996) A digital model of trabecular bone. J Bone Miner Res 11:480–489
15. Müller R, Rüegsegger P (1996) Analysis of mechanical properties of cancellous bone under conditions of simulated bone atrophy. J Biomech 29:1053–1060
16. Sugita H, Oka M, Toguchida J, Nakamura T, Ueo T, Hayami T (1999) Anisotropy of osteoporotic cancellous bone. Bone 24:513–516
17. Majumdar S, Kothari M, Augat P, Newitt DC, Lin JC, Lang T, Lu Y, Genant HK (1998) High-resolution magnetic resonance imaging: three-dimensional bone architecture and biomechanical properties. Bone 22:445–454
18. Engelke K, Graeff W, Meiss L, Hahn M, Delling G (1993) High spatial resolution imaging of bone mineral using computed microtomography. Comparison with microradiography and undecalcified histologic sections. Invest Radiol 28:341–349
19. Geraets WG, Van der Stelt PF, Lips P, Elders PJM, Van Ginkel FC, Burger EH (1997) Orientation of the trabecular pattern of the distal radius around the menopause. J Biomech 30:363–370
20. Engelke K, Dix W, Graeff W (1991) Quantitative microtomography and microradiography of bones using synchrotron-radiation. Presented at 8th International Workshop on Bone Densitometry, Bad Reichenhall, Germany
21. Rüegsegger P, Koller B, Muller R (1996) A microtomographic system for the nondestructive evaluation of bone architecture. Calcif Tissue Int 58:24–29
22. Hildebrand T, Rüegsegger P (1997) Quantification of bone microarchitecture with the structure model index. Comp Methods Biomech Biomed Eng 1:15–23
23. Jiang Y, Zhao J, Recker RR, Draper MW, Genant HK (2000) Longitudinal changes between premenopausal and postmenopausal in three-dimensional trabecular microstructural characteristics of human iliac crest bone biopsies. J Bone Miner Res 15: S184
24. Mosekilde L (1993) Vertebral structure and strength in vivo and in vitro. Calcif Tissue Int 53:S121–S125
25. Jiang Y, Zhao J, Eriksen EF, Genant HK (2003) Reproducibility of micro-CT quantification of 3D microarchitecture of the trabecular and cortical bone in the iliac crest of postmenopausal osteoporotic women and their treatment with teriparatide [rhPTH(1-34)]. RSNA 2003:571
26. Zhao J, Jiang Y, Vedi S, Compston JE, GenantT HK (2002) Longitudinal changes in three-dimensional trabecular microarchitecture of paired iliac crest bone biopsies before and after estrogen replacement therapy in postmenopausal women. J Bone Miner Res 17:S208
27. Borah B, Ritman EL, Dufresne TE, Liu S, Chmielewski PA, Jorgensen SM, Reyes DA, Turner RT, Phipps RJ, Manhart MD, Sibonga JD (2004) Five year residronate therapy normalizes mineralization: synchrotron radiation μCT study of sequential triple biopsies. J Bone Miner Res 19:S308
28. Dempster DW, Cosman F, Kurland E, Muller R, Nieves J, Woelfert L, Shane E, Plavetic K, Bilezikian J, Lindsay R (2000) Two- and three-dimensional structural analysis of paired biopsies from osteoporotic patients before and after treatment with parathyroid hormone. J Bone Miner Res 15:S194
29. Jiang Y, Zhao J, Genant HK, Dequeker J, Geusens P (1997) Long-term changes in bone mineral and biomechanical properties of vertebrae and femur in aging, dietary calcium restricted and/or estrogen-deprived/-replaced rats. J Bone Miner Res 19:820–831
30. Jiang Y, Zhao J, Prevrhal S, Genant HK (1999) Three-dimensional trabecular microstructure, bone mineral density, and biomechanical properties of the vertebral body of ovariectomized rats with estrogen replacement therapy. J Bone Miner Res 14(S1): S534
31. Zhao J, Jiang Y, Genant HK (2000) Three-dimensional trabecular microstructure and biomechanical properties and their relationship in different bone quality models. Radiology 217(P):411
32. Zhao J, Jiang Y, Prevrhal S, Genant HK (2000) Effects of low dose long-term sodium fluoride on three-dimensional trabecular microstructure, bone mineral, and biomechanical properties of rat vertebral body. J Bone Miner Res 15:816
33. Turner CH, Hsieh YF, Muller R, Bouxsein ML, Rosen CJ, McCrann ME, Donahue LR, Beamer WG (2001) Variation in bone biomechanical properties, microstructure, and density in BXH recombinant inbred mice. J Bone Miner Res 16:206–213
34. He B, Jiang Y, Zhao J, Genant HK, Goltzman D, Karaplis AC (2000) Quantitative assessment of three-dimensional trabecular bone microstructure in PTHrP wild type and heterozygous-null mice using micro computed tomography. J Bone Miner Res 15: S186
35. Takeshita S, Namba N, Zhao J, Jiang Y, Genant HK, Silva MJ, Brodt MD, Helgason CD, Kalesnikoff J, Rauh MJ, Humphries RK, Krystal G, Teitelbaum SL, Ross FP (2002) SHIP-deficient mice are severely osteoporotic due to increased numbers of hyperresorptive osteoclasts. Nat Med 8:943–949
36. Bergo MO, Gavino B, Ross J, Schmidt WK, Hong C, Kendall LV, Mohr A, Meta M, Genant H, Jiang Y, Wisner ER, Van Bruggen N, Carano RA, Michaelis S, Griffey SM, Young SG (2002) Zmpste24 deficiency in mice causes spontaneous bone fractures, muscle weakness, and a prelamin A processing defect. Proc Natl Acad Sci USA 99:13049–13054
37. Chen D, Qiao M, Story B, Zhao M, Jiang Y, Zhao J, Feng J, Xie Y, Huang S, Roberts A, Karsenty G, Mundy G (2003) BMP signaling through the Smad1 pathway is required for normal postnatal bone formation. J Bone Miner Res 18:S6
38. Zhao J, Jiang Y, Shen V, Bain S, Genant HK (2000) μCT and pQCT assessments of a murine model of postmenopausal osteoporosis and estrogen therapy. Osteoporosis Int 11(S3):S11
39. Van Rietbergen B (2003) Finite element modeling. In: Abstract Book of the 1st μCT User Workshop, Philadelphia, PA
40. Han B, Brodie T, Shen Y, Triantafillou J, Scates P, Willams J (2001) Subchondral bone changes in an ACLT model of osteoarthritis in the dog. In: Proceedings, International Symposim on Bone Biotechnology and Histotechnology, Phoenix, AZ, March 7–10, 2001, p 31

41. Bonse U, Busch F, Gunnewig O, Beckmann F, Pahl R, Delling G, Hahn M, Graeff W (1994) 3D computed X-ray tomography of human cancellous bone at 8 μm spatial and 10^{-4} energy resolution. Bone Miner 25:25–38
42. Smith CB, Silver MD (1994) Comparison between single slice CT and volume CT. In: Czichos HCH, Schnitger D (eds) International Symposium on Computerized Tomography for Industrial Applications, Bundesministerium des Innern, Bundesanstalt fur Materialforschung und-prufung, Berlin, Germany, 8–10 June, 1994
43. Holdsworth DW, Robarts JP, Thornton MM (2001) Validation of cone-beam reconstruction for bone micro-CT. In: Proceedings, International Symposim on Bone Biotechnology and Histotechnology, Phoenix, AZ, March 7–10, 2001, p 33
44. Grodzins L (1983) Optimum energy for x-ray transmission tomography of small samples. Nucl Instrum Methods 206:541–543
45. Peyrin F, Salome M, Cloetens P, Ludwig W, Ritman, Ruegsegger P, Laval-Jeantet AM, Baruchel J (1998) What do micro-CT examinations reveal at various resolutions: a study of the same trabecular bone samples at the 14, 7, and 2 micron level. Presented at the Symposium on Bone Architecture and the Competence of Bone, Ittingen, Switzerland
46. Lane NE, Thompson JM, Strewler GJ, Kinney JH (1995) Intermittent treatment with human parathyroid hormone (hPTH[1-34]) increased trabecular bone volume but not connectivity in osteopenic rats. J Bone Miner Res 10:1470–1477
47. Lane NE, Haupt D, Kimmel DB, Modin G, Kinney JH (1999) Early estrogen replacement therapy reverses the rapid loss of trabecular bone volume and prevents further deterioration of connectivity in the rat. J Bone Miner Res 14:206–214
48. Kinney JH, Haupt DL, Balooch M, Ladd AJ, Ryaby JT, Lane NE (2000) Three-dimensional morphometry of the L6 vertebra in the ovariectomized rat model of osteoporosis: biomechanical implications. J Bone Miner Res 15:1981–1991
49. Flynn MJ, Seifert HA, Irving TC, Lai B (2001) Measurement of bone mineralization in whole trabeculae using 3D x-ray microtomography. In: Proceeding of International Symposim on Bone Biotechnology and Histotechnology. Phoenix, March 7–10, 2001, p 28